MONITORING OF OFFSHORE WIND TURBINES UNDER WAVE AND WIND LOADING DURING INSTALLATION

Aljoscha Sander[1], Christian Meinhardt[2], and Klaus-Dieter Thoben[1]

[1] University of Bremen
Badgaststeiner Strasse 1, 28359 Bremen, Germany
e-mail: {aljoscha.sander,thoben}@uni-bremen.de

[2] GERB Schwingungsisolierungen GmbH & Co. KG
Roedernallee 174-176 13407 Berlin, Germany
e-mail: christian.meinhardt@gerb.com

Keywords: oscillations, offshore installation, tuned mass damper

Abstract. *During the single blade installation of offshore wind turbines, relative motion between the blade root and turbine hub can cause a delay in the progression of the installation. This contribution presents the results of a monitoring campaign conducted during the installation of an offshore wind park in the North Sea. The campaign covered different states of the turbines: without rotor blades, with rotor blades, without supplementary damping system and with an installed, tuned mass damper system. The objective of the campaign was to determine the dynamic behaviour of the turbines in correlation with wind and wave data and to determine modal parameters. Accordingly, the turbines have been instrumented with sensors to record accelerations at three different positions. The modal parameters were then obtained using SSI/FDD algorithms. Structural damping is additionally determined with an RDM algorithm, and the results are being compared. The analysis of the data will be presented, including the different stages of the structural damping and the corresponding changes in movement patterns. The results shall be used to verify the load models and the predicted response of the structure.*

1 INTRODUCTION

Offshore wind turbines are steadily increasing in size in order to meet the rising demand for green electricity. This increase in accompanied with increasing water depth of offshore wind farms. Additionally, monopiles have become the economic foundations of choice. This current state of offshore wind farms results in eigenfrequencies between 0.2 Hz and 0.3 Hz, making the offshore wind turbines more susceptible for wind and wave induced loads. The response of these turbines is dependent on geometrical as well as structural parameters, among which the structural damping is essential for fatigue loads. Therefore it is of paramount importance to accurately predict the damping of a turbine in the design phase. Offshore wind turbines have generally a low damping ratio, with typical values around 1 %. Different types of damping can be distinguished in a offshore wind turbine: structural, soil, hydrodynamic and aerodynamic damping. Additionally, for a fully operational turbine, a directional dependency of their structural behaviour due to the damping effect of aerodynamic thrust generated by the blades can be observed. Hence, side-side deflection is in general more prone to large deflection amplitudes.

Damgaard et al. (2013) [1] and Guillaume et al. (2013) [2] used acceleration measurements conducted on operational wind turbines to calculate structural damping for the different modes of tower oscillations seen in offshore wind turbines. Both oscillations due to rotor stop tests as well as oscillations under ambient conditions proved to be sufficient to get accurate enough estimates of damping ratios. As the different modes of a wind turbine are spaced very close to each other, a coupling of the two lowest eigenmodes can be assumed and therefore pure fore-aft and side-side modes are not to be expected as energy will be transformed from one mode to another. This can results in a orbit like motion, where the turbines switches oscillation directions. In order to reduce fatigue loads and subsequently increase reliability, different types of damping systems have been proposed to reduce loads in offshore wind turbines, among which are: passive, semi-active and active tuned mass dampers (TMD), tuned liquid column damper, viscous fluid dampers & magnetorheological dampers [3].

Brodersen et al. [4] investigated an active tuned mass damper implemented into HAWC2 simulations, exploring the influence of the damper on structural responses. They showed, that fore-aft oscillations behave differently compared to lateral oscillations as the blades act as 'aerodynamic dampers'. They concluded, that an active tuned mass damper needs less mass to achieve high damping, however, the damper needs to be properly tuned in order to achieve maximum efficiency. A limiting factor of the active mass damper is the displacement velocity of the damper's mass. The authors address the tuning problem, by presenting a tuning algorithm. However, external loads in offshore wind turbines are complicated by wind-wave misalignment. One mitigation might be a tuned mass damper. Steward and Lackner [5] used simulations to demonstrate that an optimally tuned mass damper can reduce fore-aft and side-side fatigue loads by 5 % and 40 % respectively for the 5 MW NREL turbine. These results were obtained by implementing a custom-written extension of FAST to include the modelling of TMDs. The authors further investigated two different orientation patterns of the TMDs. They conclude, that TMDs are cost-efficient and simple and conclude, that due to reduced loads, an increase in reliability can be expected.

Oscillations are not only critical regarding fatigue loads; relative motion between rotor hub and blade root during single blade installation can cause severe delays and thus increase cost significantly. Relative motion can be caused by aerodynamically induced movement of the blade dangling from the crane hook or by tower oscillations which in turn are caused by wind and wave loading and are thus a stochastic processes by nature. Recent work has investigated the

aerodynamic behaviour of turbine blades during craning operations in order to better understand limitations imposed by external factors such as wind speed and direction. For wind speeds between 8 - 12 m/s single blade installation was found to be feasible [6]–[9].

Jiang et al. [10] modelled the overall system consisting of a Tower-Nacelle-Hub assembly subjected to metocean loads as well as a blade under wind loading during single blade installation using HAWC2. Adapting a custom, integral criteria to assess likelihood of an installation attempt to succeed. The authors concluded, that during the final mating process between blade root and hub, tower oscillations are more dominant than blade root movements if significant resonance responses of the structure due to wave loading are present. Subsequently Jiang (2018) [3] proposed to use TMDs during the installation of offshore wind turbines at the tower top of an offshore wind turbine to reduce relative motion between blade root and nacelle hub [3]. Adapting the simulations from the previous study, the author found a 50 % reduction in relative motion when only considering the hub movement and an overall reduction of 30 % when considering both hub and blade root motion. First to demonstrate the theoretical application of an TMD for single blade installation.

Within this work, we present first measurements of a tuned mass damper used to reduce tower oscillations during single blade installation in the North Sea. Different states of the turbine undergoing installation were monitored: Tower (T), Tower, Nacelle and Hub (TNH) and Tower, Nacelle and Hub with the blades added consecutively (TNHB1, TNHB2 and TNHB3, where the number corresponds to the number of blades installed). The objective of the campaign was to monitor overall dynamic system behaviour and to obtain modal parameters.

2 MATERIAL AND METHODS

2.1 Wind farm details

A wind farm consisting of 32 multi-megawatt offshore wind turbines was installed during the time period of one year in the North Sea. The turbines have a hub height of approximately 110 m and were installed using a state of the art installation jack-up unit (IJU). The turbines are of hard-soft type and were installed in water depths between 35 m and 40 m.

The general installation procedure is as follows: (1) the IJU reaches the installation site, jacks up and connects to the previously installed transition piece atop the monopile with a gangway. (2) Following preparation on the transition piece, the tower is lifted from the IJU and placed on the transition piece. (3) The tower is followed by the nacelle-hub assembly. (4) If the conditions are favourable the blades are then installed using a specialized yoke, henceforth denoted as single blade installation tool (SBIT) with a net mass of approx. 70 t. (4.1) The SBIT is hooked onto the crane and grabs a blade from the blade rack aboard the IJU. (4.2) The SBIT and the blade are lifted to hub height and slowly manoeuvred such that the blade main axis and the generator axis are perpendicular towards each other. (4.3) Using a guiding pin, the blade root is then slowly mated with the hub flange. This processes is then repeated for each blade. It is within this phase of installation, where relative motions between blade root and hub must be at a minimum.

As this process is highly sensitive to relative motions between blade root and rotor hub a tuned mass damper was installed inside the nacelle. The TMD has two degrees of freedom and a damping mass of 10 tonnes. Using spring elements and viscous damping, the TMD was tuned to match the eigenfrequency of the turbines during single blade installation.

As the tuned mass damper was only available during the second half of the installation campaign, measurements of single blade installation with and without a TMD were conducted.
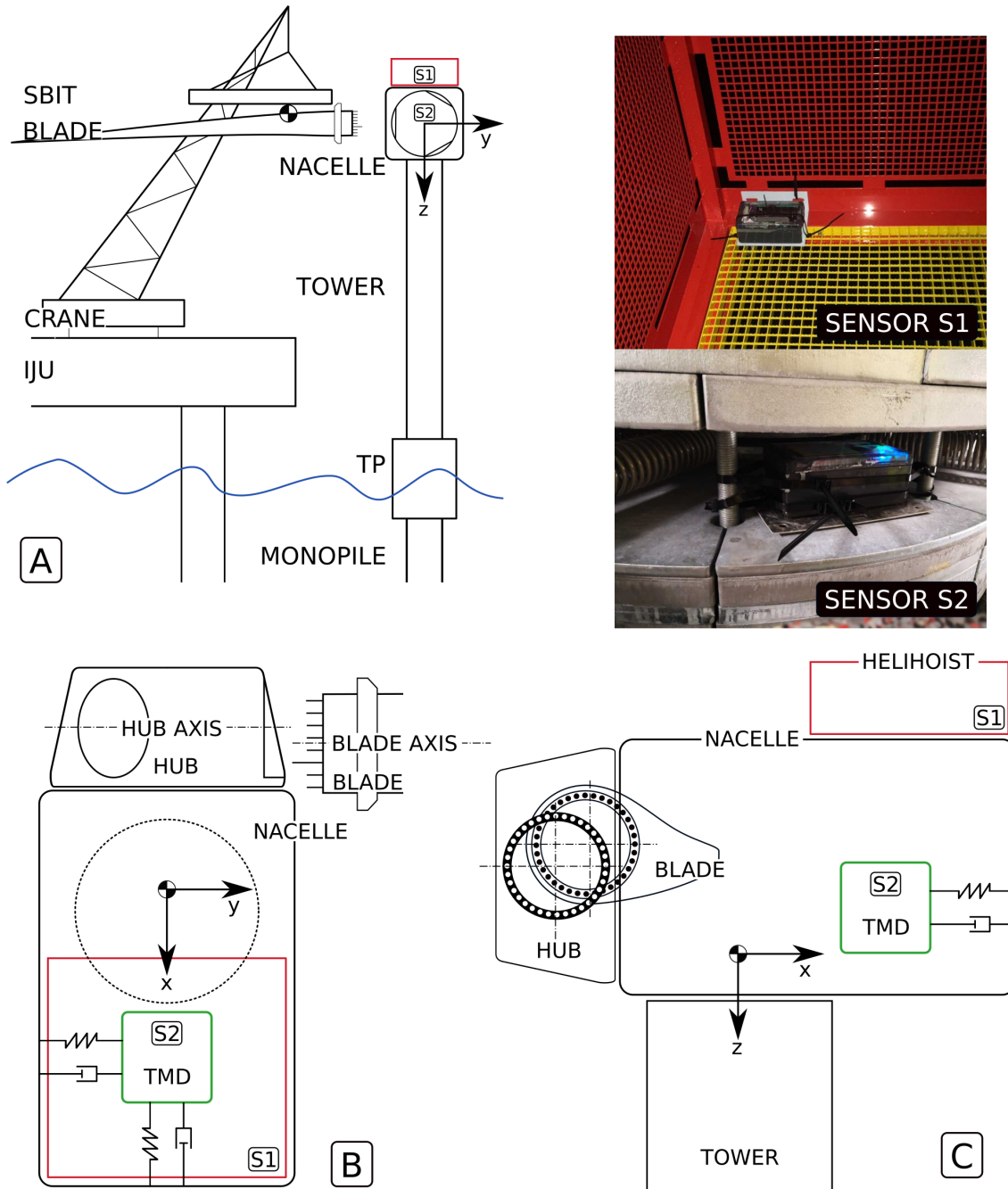
Figure 1: Typical setup of a single blade installation. (A) Installation Jack Up Unit (IJU) next to the Tower-Nacelle-Hub Assembly with the blade being attached to a Single Blade Installation Tool (SBIT), typically a yoke-like structure. The red square indicated the helicopter hoisting platform. S1 and S2 correspond to the sensors used within this study to determine dynamic behaviour of the turbine. (B) Top view of the single blade installation process. The green structure represents the tuned mass damper, deployed during single blade installation. (C) Side view of the installation process. Upper right figures: Sensors S1 and S2 mounted on the helicopter hoisting platform and the tuned mass damper respectively.

2.2 Measurements

In order to monitor the dynamic behaviour of the turbines during installation, custom build sensor boxes were deployed at two different positions: one sensor box is placed on the topmost position of the nacelle: the helicopter hoisting platform (short: helihoist). A second sensor box is placed on the tuned mass damper during installations where a tuned mass damper was present.

Sensor boxes contained a lead battery and electronics in a water proof containment (box) with a weight of approximately 3 kg and the measurements of 0.2 m x 0.06 m x 0.1 m. A LSM9DS1 (SparkFun Electronics, Colorado, USA) 9-Degrees-of-Freedom inertial measurement sensor capable of measuring linear acceleration, linear angular acceleration and the magnetic field was combined with a GPS-Sensor (GP-20U7; SparkFun Electronics, Colorado, USA), providing accurate time stamps as well as altitude information to form the sensory core of the sensor boxes. A real time clock (RS3231) provided back up temporal information in case of lack of GPS signal. A 32 GiB micro-SD-Card was used to store measurements. As a microcontroller, an ESP32 (Espressif Systems, Shanghai, China) was used. A sample frequency of 33 Hz was used, yielding accurate temporal resolution while allowing for good battery run time.

A LiDAR aboard the IJU provided high spatial and temporal resolution wind field information (measurement return period 1 s / 1 Hz). Additionally, a wave buoy in the vicinity of the installation site provided wave data, including significant wave height, peak period, zero upcrossing period and wave direction. The measurement return period was 30 min. / 0.00055 Hz.

In total, 15 turbines without a TMD and 4 turbines with a TMD were monitored during installation.

2.3 Data processing

All data post-processing has been implemented utilizing Python3 as well as it's rich set of scientific data analysis frameworks. As a fundamental data structure Pandas DataFrames (version 0.24.2) [11] was used. Numerical calculations were carried out using NumPy version 1.16.4 [12] and SciPy, version 1.3.0 [13]. All figures were generated using Matplotlib version 3.1.0.

Post-processing of measurement data starts with the subtraction of the mean for each acceleration component. Accelerations were then resampled using a linear interpolation scheme to a constant frequency of 30 Hz and filtered using a Butterworth Bandpass filter of third order. Lower and upper cut off frequencies were set to 0.1 and 1 Hz respectively. Accelerations were then integrated twice to yield velocity and position of the sensors during installation. Integration was carried out by applying a second order trapezoid scheme utilizing SciPy's integation module.

Based upon the positional vector, the instantaneous tower deflection D was calculated:

$$D = \sqrt{x^2 + z^2} \tag{1}$$

Where x and z are the instantaneous position vector components. The second component of the positional vector has been omitted, as it is aligned parallel to the tower axis and therefore it's contribution to the tower top deflection can be neglected.

To obtain a measure for the current state of the turbine and to allow for correlations with environmental data, 10 minute means of D were calculated, denoted as D_{10}. To maintain OEM privacy, all data has been normalised by the turbine tower diameter d_T, such that: $d = D/D_T$

and $d_{10} = D_{10}/D_T$. To further enhance privacy all dates presented in this study have been reset such that all measurements start at 01.01.1970 at 00:00 UTC. Temporal information is therefore only relative.

Wind data was binned into 10 minute windows and the window average was calculated. For wave measurements, data was first upsampled to 10 minute periods utilizing a forward interpolation scheme and subsequently merged with the wind data. Figure 2 depicts the data processing steps.

Figure 2 shows the data processing pipeline. Raw data is resampled, filtered and integrated twice to yield both velocity and position of the sensor in space and time. Using the postion vector, the deflection of the Nacelle can be calculated by employing Equation 1. Combining these measurements with metocean data and applying temporal averaging allows for scatter plots of mean deflection and metocean parameters such as significant wave height.
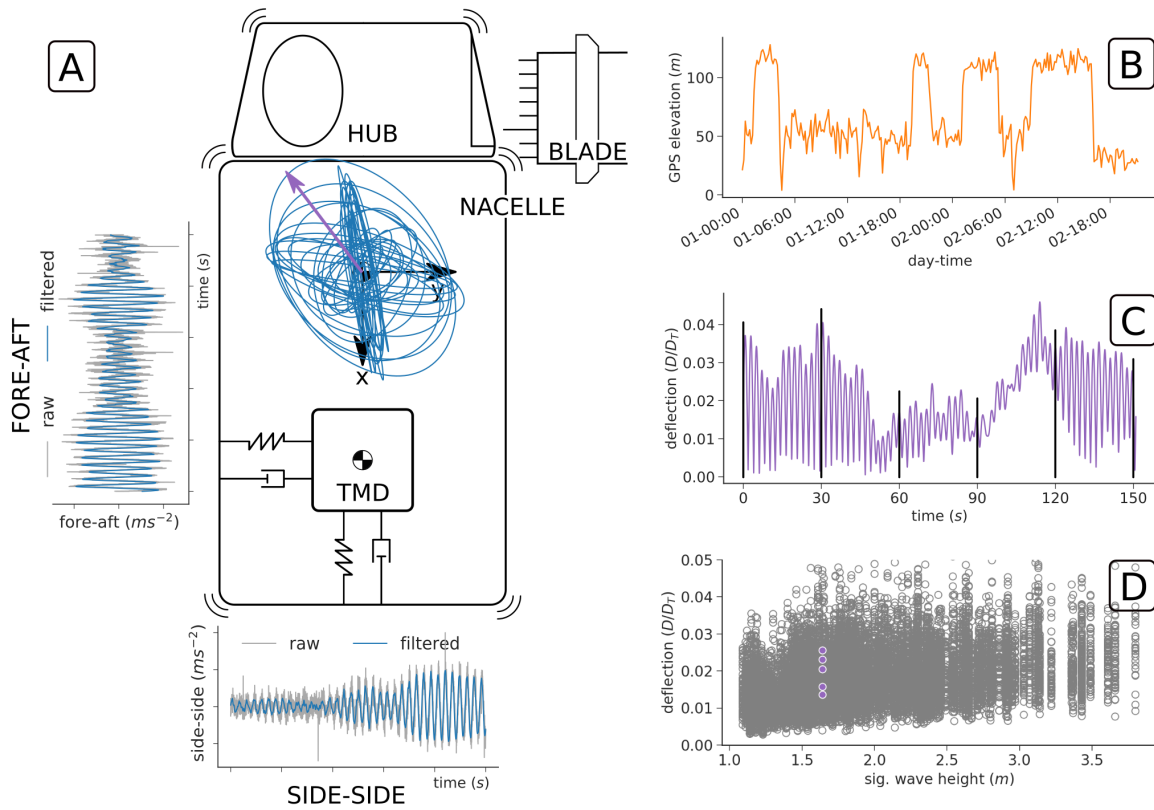
Figure 2: Data acquisition and processing: (A) Fore-aft and side-side accelerations are recorded by the sensors, resulting in a trajectory which can swiftly change direction. (B) GPS-Profile of the single blade installation process captured by another sensor mounted on the single blade installation tool. This allowed accurate tracking of the process in both space and time. (C) Integration of accelerations yields the trajectory of the orbit, from which the absolute deflection, a measure of how much the nacelle diverges from its base position can be obtained. (D) Applying a 60 s average of the deflection allows for the correlation of the deflection with external parameters, such as sig. wave height or wind speed.

2.4 Modal parameters

The monitoring campaign, which covered the states where the tuned mass damper system was either disabled (blocked) or activated was also used to identify the effectiveness of the TMD system by continuously determining the overall structural damping of the Tower-Nacelle-Hub assembly. To determine the structural damping ratio from the accelerations with unknown input (output only data), system identification techniques are applied such as the Random Decrement Method (RDM) as well as Stochastic Subspace Identification (SSI) and Enhanced Frequency Domain Decomposition (EFFD).

Random Decrement Method   Figure 3a schematically shows the principle behind the random decrement method. Based on the assumption that the random excitation consists of a deterministic component which corresponds to free vibration terms and a random component which corresponds to forced vibrations, the random part can be eliminated by averaging a large number of blocks extracted from the time domain signal with a length τ. The blocks are chosen with the help of a threshold level. The Random Decrement Signature (RDS) (Figure 3b and Figure 3c) results the averaged time segments and the resulting damping ratio can be derived from the logarithmic decrement whereas the quality of the RDS strongly depends on the selection of the segment duration τ and the threshold y_S.

The random decrement method has been approved for system identification analyses of structures and buildings ([14]–[16]). Since the results of the damping are depending on the threshold and the segment duration, these parameters were varied to gain stochastic certainty. A window length of 2 and 3 periods (based on the determine natural frequency of the main structure) was analysed as well as a threshold level of 30 %, 50 % and 60 % of the max value of the investigated time history.

Figure 3b and Figure 3c show exemplary random decrement signatures from which the structural damping of the TNH was determined by analysing the decaying curve. This process was automated and applied for the complete time series that were recorded.

Operational Modal Analysis   The stochastic subspace identification method is considered as a robust output-only identification technique compared to other available methodologies [17]. SSI algorithms identify a stochastic state-space model of the structure. The resulting model can then be translated into a more convenient structural model form for engineering interpretation of the results. The state-space model can be related to both modal model and Finite Element (FE) model formulations. The method works in the time domain and is based on a state space description of the dynamic problem assuming a linear behavior of the structure and a time-invariant dynamic response of the system due to a white-noise excitation. The system identification results at different model orders are compared to distinguish true structural modes from spurious modes in so-called stabilization diagrams. The time domain based SSI technique together with additional techniques such as the Enhanced Frequency Domain Decomposition (EFDD) techniques are often combined in algorithms for commercial Operational Modal Analysis software packages. The EFDD method relies on computation of response spectra. Long records are, therefore, required to keep low the error on spectrum estimation and to extract modal parameters in a reliable way. The software ARTEMIS from SVIBS (Structural Vibration Solutions) was used to identify the vibration modes of the TNH and to determine the structural damping. The results are plotted as stabilization cards and the estimated modal parameters are listed together with information about the probabilistic uncertainty.
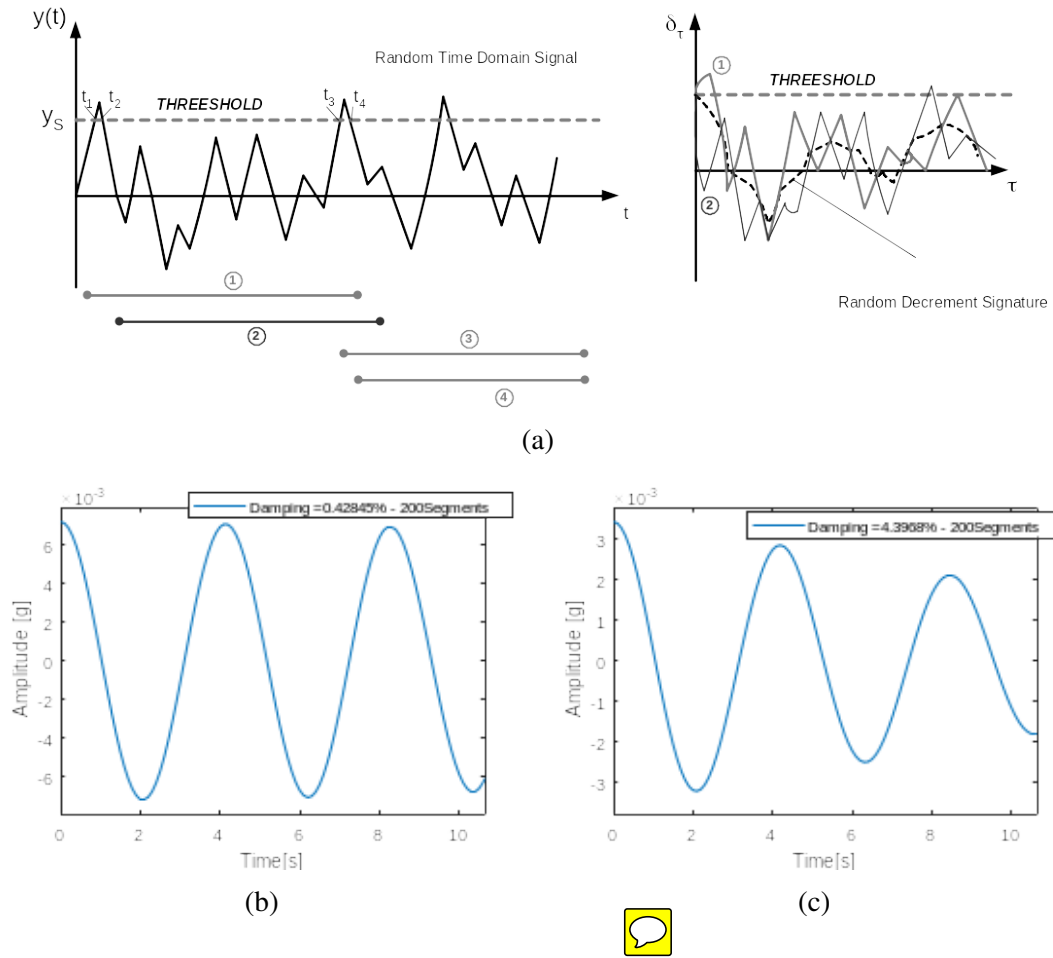
(a)

(b)

(c)

Figure 3: Principle of the Random Decrement Method (a). (b) Random Decrement Signature (RDS) of a 10 minute time history segment with blocked TMD – (c) (RDS) of a 10 minute time history segment with activated TMD

Identification of TMD parameters   A two-measuring point acquisition, for which the vibrations of the wind turbine tower structure and the vibrating mass of the TMD are recorded can be used to determine the TMD parameters. But since this method will only provide the absolute vibrations of main structure and TMD a certain post-processing effort is required. Direct information regarding the relative TMD displacements can be gained when the relative vibrations of the TMD mass in addition to the vibrations of the main structure are getting obtained to derive the TMD parameters directly.

3   RESULTS

3.1   Nacelle deflections during single blade installation

Figure 4 shows exemplary two time series of nacelle deflection during the installation of two offshore wind turn turbines during single blade installation, where one turbine was equipped with a tuned mass damper. Both instantaneous deflection as well as the 10 min. mean of the deflection is shown (white line). A black horizontal line indicates the limit for single blade installation as learned during previous installations. For the installation without a TMD (Figure 4a), this limit is exceeded multiple times, Though the 10 min. average remains well below the limit. The time series shown starts after the finalised nacelle installation, spans an intermediate time period of about two hours within which the single blade installation tool (yoke) is picked up by the crane and then includes the three consecutive blade installations. Total blade installation spanned approx. 62 h with installation attempts made at each window where the deflection dropped below 3 % tower diameter. Six attempts at blade installation were made, for each blade two, where each of the first attempts failed.

During single blade installation with a TMD (Figure 4b) deflection was almost entirely above the threshold. With the beginning of the blade installation, the TMD was activated. This is indicated by the hatched area. An immediate response in nacelle deflection can be observed with the instantaneous deflection dropping below the installation limit with the exception of four spikes. The 10 min. mean of the nacelle deflection assumes a near constant value at when compared to the prior time period. The total blade installation installation duration was approx. 13 h, a significant reduction when compared to the previous installation duration without a TMD. To compare the two installations and to correlate the observed behaviour with metocean parameters, time series were divided into 10 min. segments and a temporal average was applied. This is shown in Figure 4c, where the 10 min. mean nacelle deflection is shown for the two previous installations as a function of the significant wave height.

During the installation without a TMD, significant wave height was between 0.75 m and 1.8 m. For the installation with a TMD, the wave range was between 1.25 m and 1.9 m. A clear reduction in mean deflection can be observed. Furthermore, while for the installation without a TMD mean deflection spread for a constant sig. wave height, spreading is significantly reduced with a TMD present.

Figure 5 shows 10 min. mean deflections for all captured installations with (red) and without (blue) a TMD present. The 10 min. mean deflection as a function of the significant wave height (Figure 5a), the wave peak period (Figure 5b) and the 10 min. mean wind speed (Figure 5c) are shown. Additionally, to give a simple model, a linear function is fitted using linear regression to both data sets.

The linear functions for both installations with and without TMD converge at a min. mean deflection of 0.5 %. For the installations with the TMD activated, the slope of mean deflection with significant wave height and wind speed is greatly reduced compared to the installations without a TMD present. As in Figure 4c, the spreading for a given wind speed Figure 5c or wave height Figure 5a is reduced as well. No clear correlation between mean deflection and wave peak period can be observed.
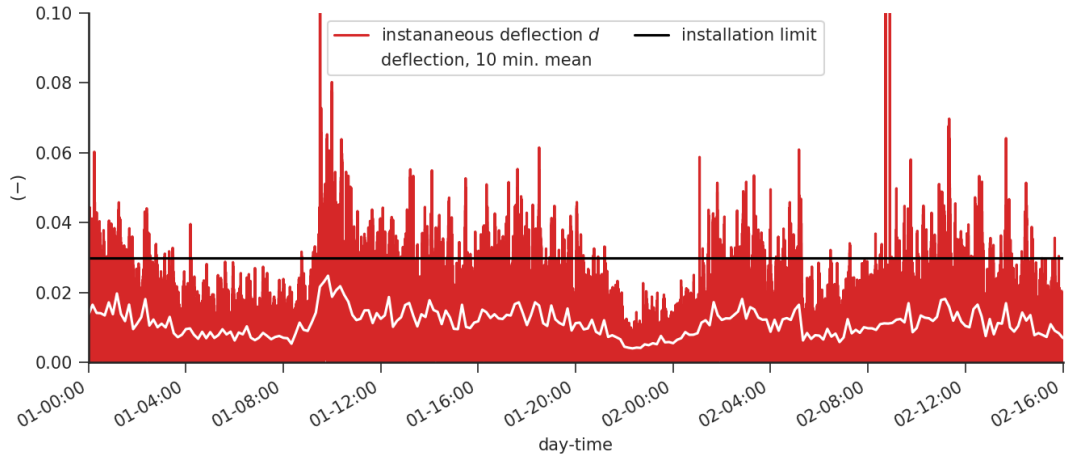
(a)
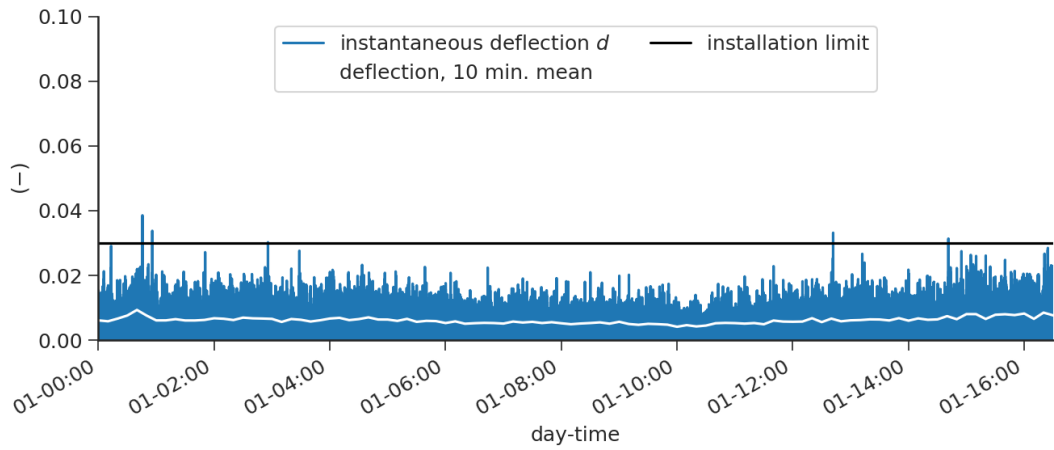
(b)
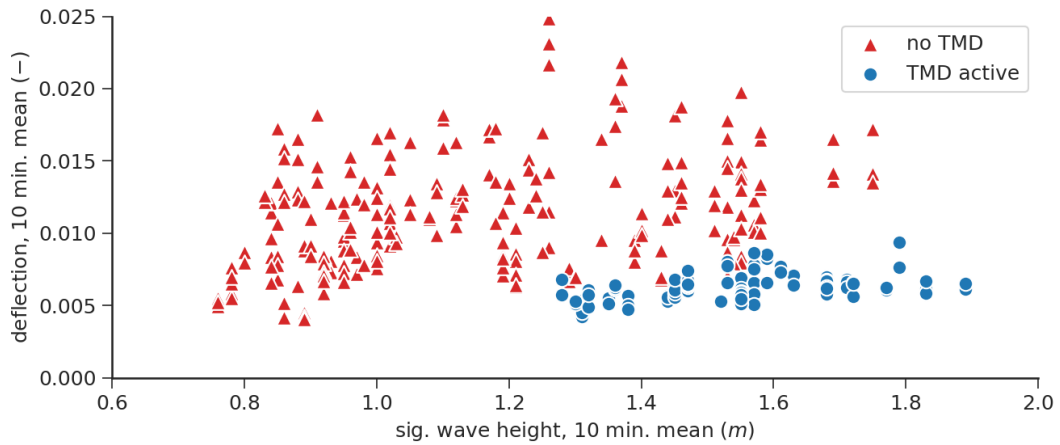
(c)

Figure 4: Time series of the nacelle deflection during single blade installation without a tuned mass damper (TMD) (a) and with TMD present (b). The white lines indicate the 10 min. mean of the deflection. The black line represents the empirically determined single blade installation limit of the deflection above which most installation attempts fail. (c) shows a scatter diagram of the 10 min. mean deflections from the two installations as a function of significant wave height.

10
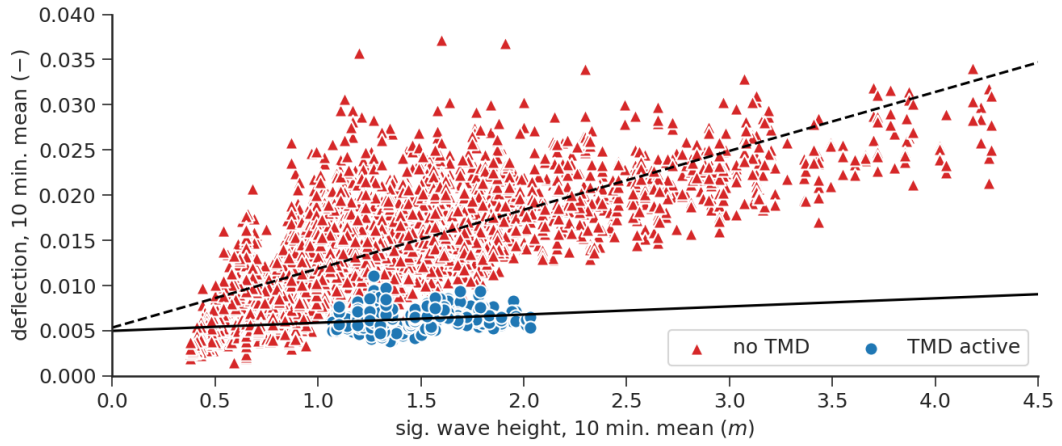
(a)
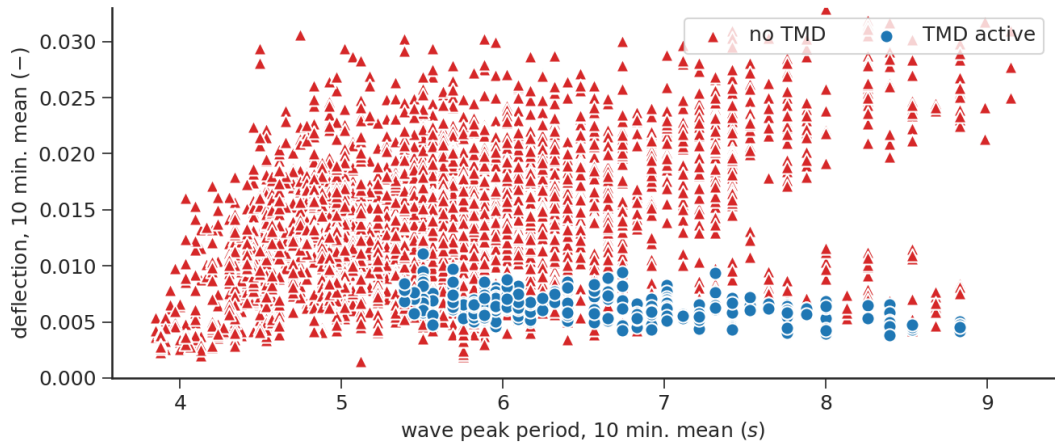
(b)
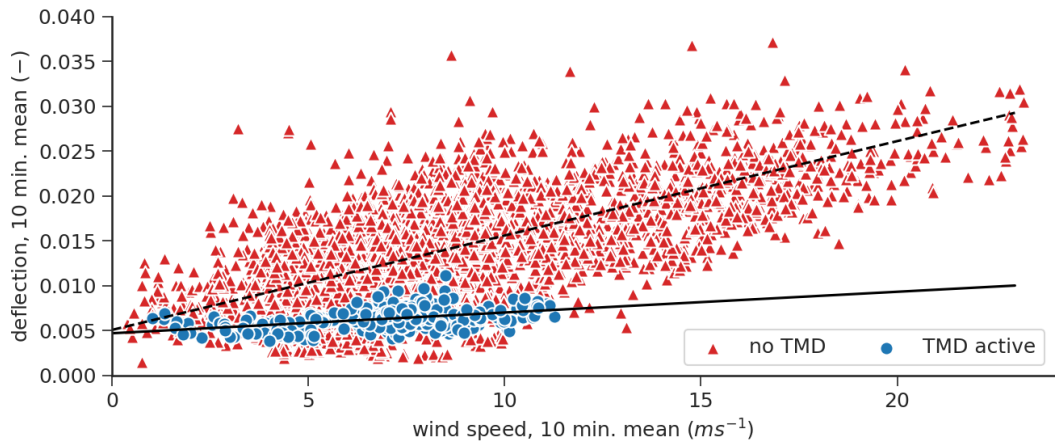
(c)

Figure 5: Scatter diagrams for the 10 min. mean deflection as a function of significant wave height H_S (a), wave peak period T_P (b) and the 10 min. mean wind speed U (c). Red indicates installations without a tuned mass damper (TMD), blue corresponds to installations with an active TMD.

11

3.2 Modal parameters

Figure 6 shows recorded time series of fore-aft and side-side accelerations of the wind turbine in different configurations (TNH, THNB1, TNHB2 and TNHB3) as well as the corresponding spectrograms (lower row, left and right hand side) which show the Auto Power Spectra of 10 minute - time segments plotted vs. the entire time of the monitoring campaign for the examined structure. The spectrogram not only indicates the times of the rotor blade installation for which a shift of the natural frequency can be detected but also the reduced acceleration values of the Auto-Power-Spectra and the much wider peaks indicating the increase of structural damping.
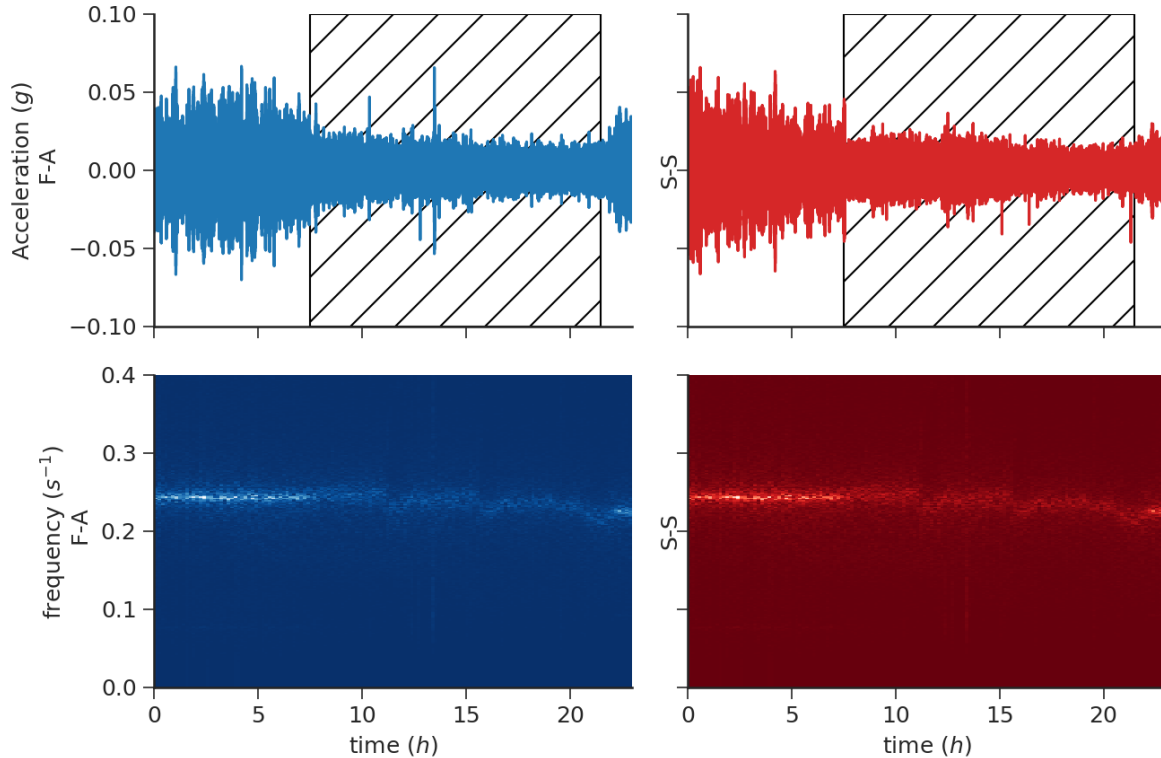

Figure 6: Top: Measured acceleration time series (fore-aft and side-side direction) of the wind turbine tower with Nacelle during single blade installation. The hatched area indicates the TMD being unlocked, resulting in an immediate reduction in accelerations. Bottom: Spectrogram (APS for 10 min time segments vs. recorded time). With each installed blade, a shift in frequency can be observed.

Figure 7 shows the determined damping ratios for time series with a length of 10 minutes, obtained via RDM. The time periods for which the TMD has been activated can clearly be identified. With the TMD deactivated, the damping ratio remains mostly below 1 %. With the activation of the TMD, damping ratio increases to values between 2 % and 4 %.

Figure 8a and Figure 8b show the resulting stabilization diagrams for a time period with blocked TMD and with activated TMD. It can be seen that for the state with blocked TMD the identified modal parameters coincide with structural damping determined with the Random Decrement Method. The damping estimation with the SSI algorithm revealed smaller structural damping ratios than determined with the RDM (TMD active: 2,52 %, no TMD: 0.57 %).
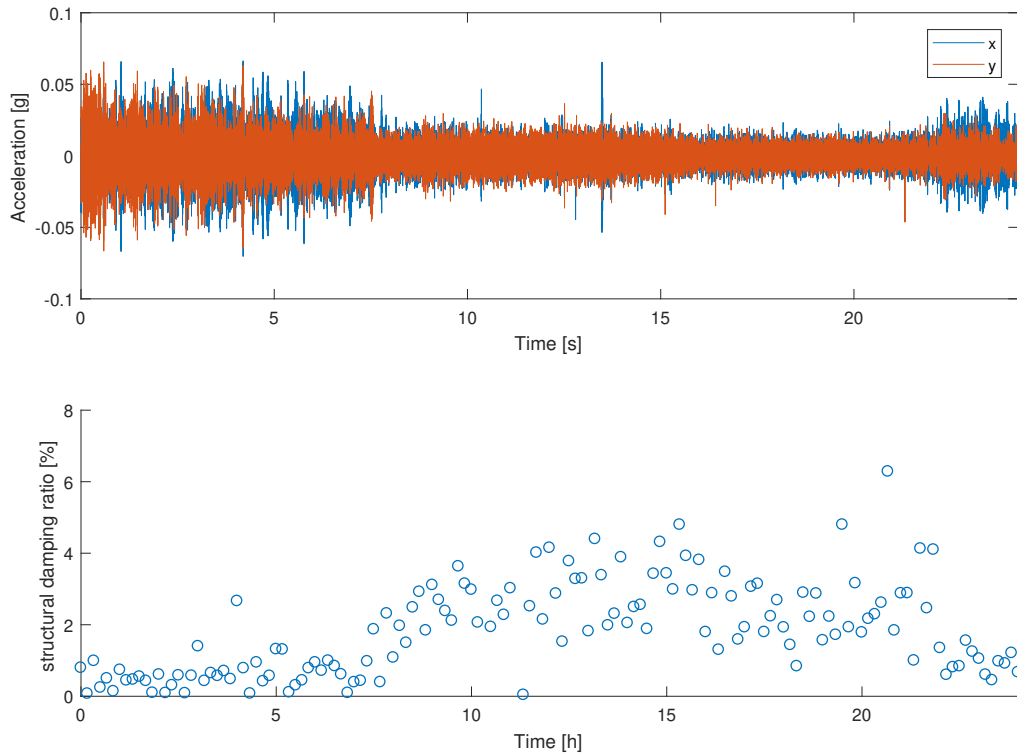
Figure 7: Above: Measured acceleration time histories of the wind turbine tower with Nacelle during rotor blade installation (x: fore-aft and y: side-side). Below: Determined Structural Damping ratio for time segments of 10 minutes using the Random Decrement Method
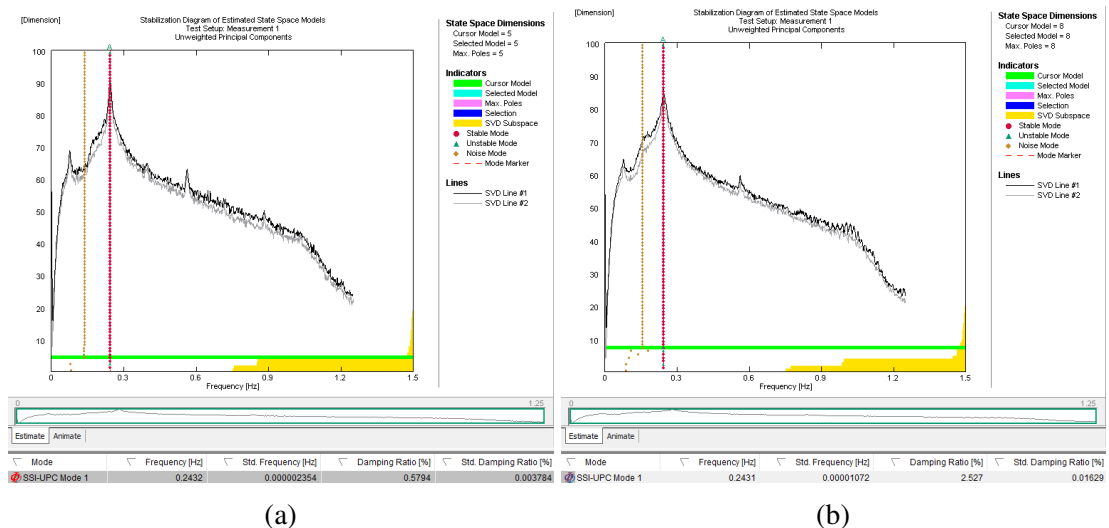

Figure 8: Resulting Stabilization Diagrams from the Operational Modal Analysis (SSI Method) using the recorded ambient accelerations of TNH during single blade installation – (a): with blocked TMD – (b): with TMD – tuning frequency higher than optimum

3.3 Behaviour of the Tuned Mass Damper

Figure 9 shows the FFT spectra of 5 minute time segments of the accelerations measured at he nacelle (left) and the TMD mass (right). Initially (Time $\leq$ 1h) the FFTs of the Nacelle and the TMD mass show the same acceleration amplitudes and similar narrow peaks, which indicates, that the TMD is blocked. Later the FFT spectra of the Nacelle shows much smaller acceleration amplitudes with wider peaks, indicating that the TMD is active.
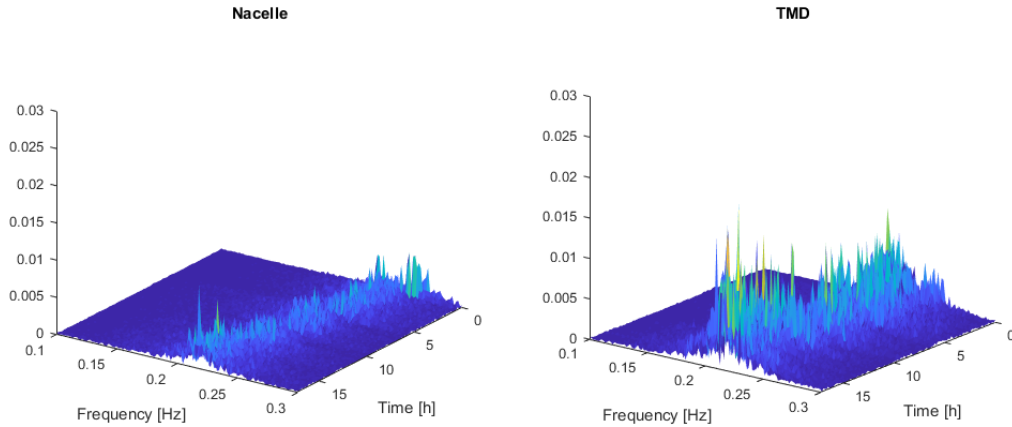

Figure 9: FFT Spectra of the acceleration time histories (5 minute segments) at Nacelle and TMD mass plotted for the entire monitoring time

The transfer function (shown for the measured accelerations of the nacelle in Figure 10) corresponds to a Frequency Response Function of the TMD system without the interaction with the main structure. From this function the tuning frequency and TMD damping ratio can is obtained by comparison with a single-degree of freedom approximation.The tuning frequency is 0.227 Hz while the TMD damping ratio is determined to be 10 %.
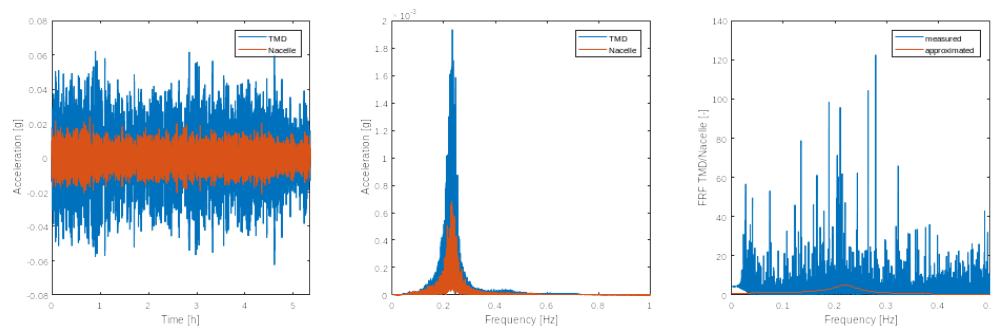

Figure 10: Left: Recorded Time Histories of the accelerations at Nacelle and TMD – Center: FTT Spectra of the entire time – Generated Transfer function and approximated signle degree of freedom - frequency response function with a tuning frequency of 0.227 Hz and a TMD damping ratio of 10 %.

4 DISCUSSION

The results presented here indicate that a TMD might indeed be a cost-effective and robust measure to improve single blade installation. However, much remains to be learned about the correlations and causalities of observed effects during single blade installation. While the measurements showed, that relative motions are indeed driven by wind and waves, the strong correlation between wind and waves - at least in the North Sea - does not allow to discern whether one of the two loads is the main driver.

While the TMD reduced deflections by more than 50 % compared to deflections observed during installations without a TMD at similar sea states other factors may still have a significant influence on the success of the single blade installation process. Among these are wind loads on the blade lifting device, wave loads on the ship and human influence as the installations are carried out manually. Structural damping increased significantly, independent on calculation method. Nevertheless more measurement with a higher precision are needed to gain more insight into the dynamic behaviour of offshore wind turbines in general and during installation in particular.

Apart from a reduction in relative motion and an increase in structural damping, the tuned mass damper increases the predictability of turbine behaviour during planning and execution of single blade installation and thus leads to a significant reduction in (financial) project risk.

Furthermore, the reduction in relative motion also leads to a reduction in HSE risks as well as a reduction in component damage. The unpredictable nacelle motions during the mating of the blade root and the hub pose a significant risk to technicians and can also lead to collisions between the hub/nacelle and the blade/lifting device.

While intended as a cost-efficient manner of measuring dynamic behaviour of the turbines during installation, it has become apparent, that the MEMS-based sensor devices are fully capable of measuring relevant parameters with the needed precision and therefore present a novelty as well. In future studies the data obtained during this measurement campaign should be used to verify design load models as well as structural responses obtain via numerical simulations.

With regards to the operational modal analysis: a trial to determine the frequency response function for shorter time periods and detect variations of the TMD parameters with varying excitation levels and characteristics was not possible, since the time periods have to be long enough to generate the transfer function for TMD and Nacelle. While measuring the accelerations of the vibrating mass of a TMD system only provides an absolute vibration value, the direct acquisition of the relative displacement between TMD mass and main structure enables to determine the resulting TMD displacement directly but again not the TMD parameters such as tuning frequency and damping. To assess these values a comparison with a calculation model is still required.

We hypothesize, that the success rate of single blade installation is also dependent on the direction of oscillations, e.g. the shape of the orbit. This has yet to be investigated in future studies, where installation times should be correlated not only with nacelle deflection but also deflection direction and changes thereof.

5 ACKNOWLEDGEMENT

References

[1] M. Damgaard, L. B. Ibsen, L. V. Andersen, and J. K. F. Andersen, "Cross-wind modal properties of offshore wind turbines identified by full scale testing," en, *Journal of Wind Engineering and Industrial Aerodynamics*, vol. 116, pp. 94–108, May 2013. DOI: `10.1016/j.jweia.2013.03.003`.

[2] P. Guillaume, G. De Sitter, P. J. Jordaens, and C. Devriendt, "Damping estimation of an offshore wind turbine on a monopile foundation," en, *IET Renewable Power Generation*, vol. 7, no. 4, pp. 401–412, Jul. 2013. DOI: `10.1049/iet-rpg.2012.0276`.

[3] Z. Jiang, "The impact of a passive tuned mass damper on offshore single-blade installation," English, *Journal of Wind Engineering and Industrial Aerodynamics*, vol. 176, pp. 65–77, May 2018, WOS:000432502100006. DOI: `10.1016/j.jweia.2018.03.008`.

[4] M. L. Brodersen, A.-S. Bjørke, and J. Høgsberg, "Active tuned mass damper for damping of offshore wind turbine vibrations," *Wind Energy*, vol. 20, no. 5, pp. 783–796, 2017.

[5] G. M. Stewart and M. A. Lackner, "The impact of passive tuned mass dampers and wind–wave misalignment on offshore wind turbine loads," *Engineering Structures*, vol. 73, pp. 54–61, 2014.

[6] M. Gaunaa, L. Bergami, S. Guntur, and F. Zahle, "First-order aerodynamic and aeroelastic behavior of a single-blade installation setup," en, *Journal of Physics: Conference Series*, vol. 524, p. 012 073, Jun. 2014. DOI: `10.1088/1742-6596/524/1/012073`.

[7] M. Gaunaa, J. Heinz, and W. Skrzypiński, "Toward an Engineering Model for the Aerodynamic Forces Acting on Wind Turbine Blades in Quasisteady Standstill and Blade Installation Situations," en, *Journal of Physics: Conference Series*, vol. 753, p. 022 007, Sep. 2016. DOI: `10.1088/1742-6596/753/2/022007`.

[8] Y. Wang, D. Tian, and W. He, "Computation of hoisting forces on wind turbine blades using computation fluid dynamics," *Applied Mechanics and Materials*, vol. 446-447, pp. 452–457, 2014. DOI: `10.4028/www.scientific.net/AMM.446-447.452`.

[9] L. Kuijken, "Single Blade Installation for Large Wind Turbines in Extreme Wind Conditions," en, Master of Science Thesis, European Wind Energy Master - TU Delft and DTU, 2015.

[10] Z. Jiang, Z. Gao, Z. Ren, Y. Li, and L. Duan, "A parametric study on the final blade installation process for monopile wind turbines under rough environmental conditions," English, *Engineering Structures*, vol. 172, pp. 1042–1056, Oct. 2018, WOS:000445440300076. DOI: `10.1016/j.engstruct.2018.04.078`.

[11] W. McKinney, "Data Structures for Statistical Computing in Python," 2010, pp. 51–56.

[12] S. van der Walt, S. C. Colbert, and G. Varoquaux, "The NumPy Array: A Structure for Efficient Numerical Computation," *Computing in Science Engineering*, vol. 13, no. 2, pp. 22–30, Mar. 2011. DOI: `10.1109/MCSE.2011.37`.

[13] SciPy 1.0 Contributors, P. Virtanen, R. Gommers, T. E. Oliphant, M. Haberland, T. Reddy, D. Cournapeau, E. Burovski, P. Peterson, W. Weckesser, J. Bright, S. J. van der Walt, M. Brett, J. Wilson, K. J. Millman, N. Mayorov, A. R. J. Nelson, E. Jones, R. Kern, E. Larson, C. J. Carey, İ. Polat, Y. Feng, E. W. Moore, J. VanderPlas, D. Laxalde, J. Perktold, R. Cimrman, I. Henriksen, E. A. Quintero, C. R. Harris, A. M. Archibald, A. H. Ribeiro, F. Pedregosa, and P. van Mulbregt, "SciPy 1.0: Fundamental algorithms for scientific computing in Python," en, *Nature Methods*, Feb. 2020. DOI: `10.1038/s41592-019-0686-2`.

[14] H. A. Cole, "On-line failure detection and damping measurement of aerospace structures by random decrement signatures," Tech. Rep., Mar. 1973.

[15] J. C. Asmussen, S. R. Ibrahim, and R. Brincker, *Random decrement : Identification of structures subjected to ambient excitation*, en, Library Catalog: www.semanticscholar.org, 1998.

[16] B. Peeters and G. De roeck, "REFERENCE-BASED STOCHASTIC SUBSPACE IDENTIFICATION FOR OUTPUT-ONLY MODAL ANALYSIS," en, *Mechanical Systems and Signal Processing*, vol. 13, no. 6, pp. 855–878, Nov. 1999. DOI: `10.1006/mssp.1999.1249`.

[17] M. Döhler, P. Andersen, and L. Mevel, "Operational Modal Analysis Using a Fast Stochastic Subspace Identification Method," en, in *Topics in Modal Analysis I, Volume 5*, R. Allemang, J. De Clerck, C. Niezrecki, and J. Blough, Eds., Series Title: Conference Proceedings of the Society for Experimental Mechanics Series, New York, NY: Springer New York, 2012, pp. 19–24. DOI: `10.1007/978-1-4614-2425-3_3`.